



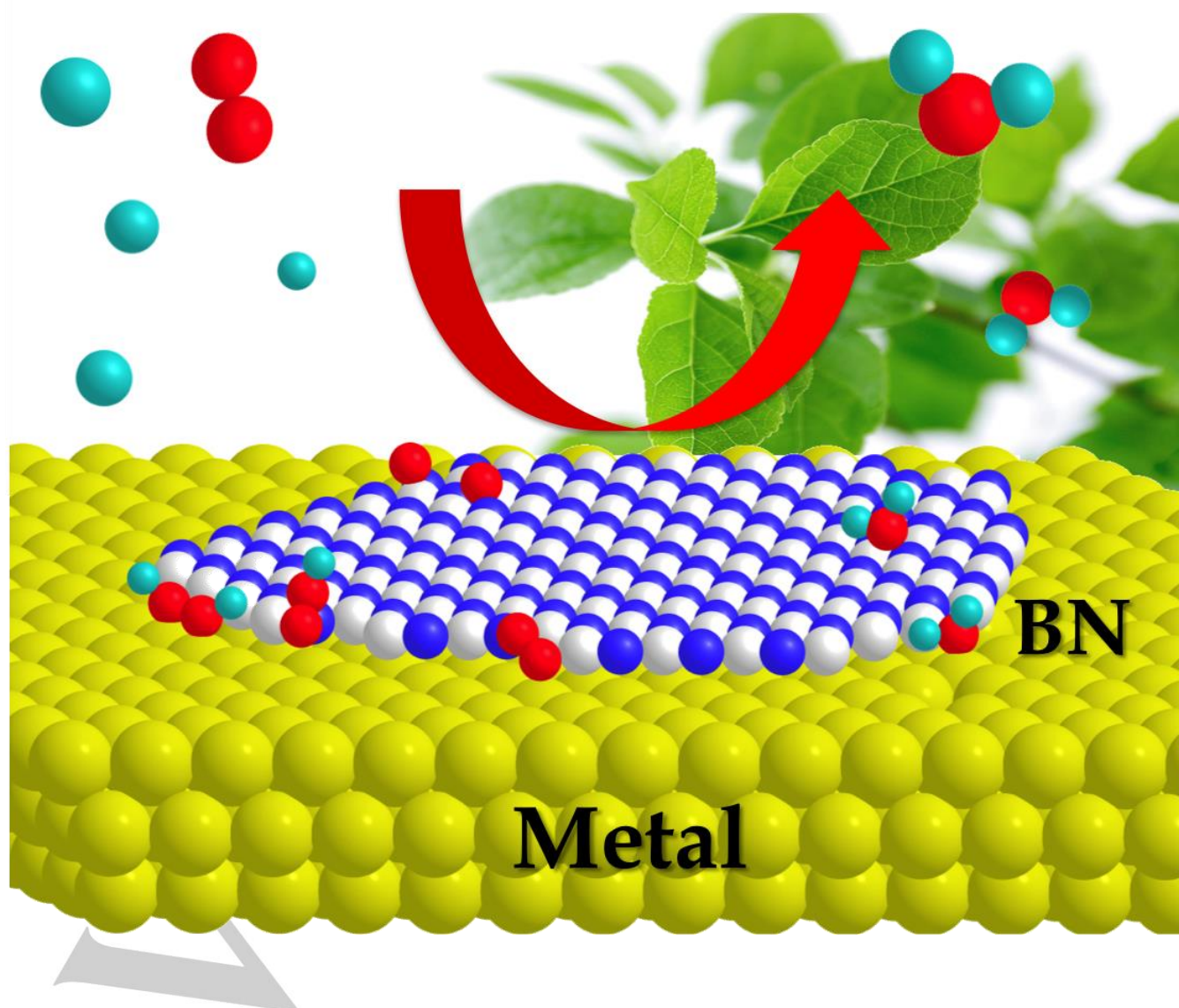
Title	When Inert Becomes Active : A Fascinating Route for Catalyst Design
Author(s)	Lyalin, Andrey; Gao, Min; Taketsugu, Tetsuya
Citation	Chemical record, 16(5), 2324-2337 https://doi.org/10.1002/tcr.201600035
Issue Date	2016-10
Doc URL	http://hdl.handle.net/2115/67239
Rights	This is the peer reviewed version of the following article: Lyalin, A., Gao, M. and Taketsugu, T. (2016), When Inert Becomes Active: A Fascinating Route for Catalyst Design. The Chemical Record, 16: 2324–2337, which has been published in final form at doi:10.1002/tcr.201600035. This article may be used for non-commercial purposes in accordance with Wiley Terms and Conditions for Self-Archiving.
Type	article (author version)
File Information	personal_account-7.pdf



[Instructions for use](#)

When inert becomes active: fascinating route for catalyst design

Andrey Lyalin,*^[a] Min Gao^{[b][c]} and Tetsuya
Taketsugu*^{[b][c]}



Abstract: In this personal account, we review the work of our group in the area of energy and environment related nanocatalysis in the past seven years. We focus on understanding the fundamental mechanisms, which control properties of atomic clusters and nanoparticles – a form of matter that is intermediate between atoms and their bulk counterpart. The emphasis is made on the theoretical design of effective catalysts based on cheap and abundant elements. The main idea that stands behind of our work is that even catalytically inactive or completely inert materials can be functionalized at nanoscale via the size, structure, morphology and support effects. Such approach opens principally new ways to design catalytically active systems based on materials never before been considered as catalysts. In particular we demonstrate that the hexagonal boron nitride (*h*-BN), which was traditionally considered as an inert material, can be functionalized and become active for a number of catalytic reactions involving oxygen activation, oxidation by molecular oxygen, and oxygen reduction reaction (ORR).

Introduction

In the last thirty years the field of nanocatalysis has undergone an explosive development.^[1, 2] Such interest in nanocatalysis is stipulated by the fact that properties of materials at nanoscale strongly depend on the size, morphology and composition of nanoparticles, support and interface effects and hence can be controlled or tuned by these factors in order to create unique materials via atom-by-atom design. Often nanoparticles demonstrate properties that are absent in the corresponding bulk or molecular systems, making realm of nanoparticles one of the most exciting area in modern physics and chemistry.

There are two different approaches towards design of novel catalytic materials. The first one is the routine experimental screening of a huge number of different compounds. Basically this is a trial and error method based on the chemical intuition and good luck. Often such method is used to improve activity of already known catalysts or to reduce amount of expensive and rare platinum group metals (PGM) which is the largest challenge for many industrial chemical processes. When such catalyst with the improved properties is found in experiments, the consequent theoretical simulations can help to explain or confirm the mechanism of catalytic reaction.

The second approach is based on the theoretical modeling and

computer simulations of the principally novel type of catalytic materials. With increase in computer power and development of the efficient and reliable theoretical methods such approach becomes very promising tool for design of solid catalysts with unique properties.^[3] Our group is working in this direction. What excite us the most in the computational approach is the possibility to model or perform computer experiment with any type of materials, even those not yet synthesized in the laboratory conditions? Theoretical methods to determine the structures of unknown materials are also available.^[4] Therefore in our group we focus on the functionality and eager to predict novel type of materials with targeted properties. Being predicted theoretically, such catalysts should always undergo experimental verification to prove and confirm their catalytic properties.

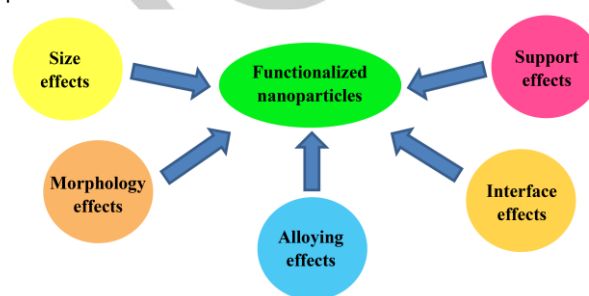


Figure 1. Variety of factors that can be used to functionalize nanoparticles and design novel nanocatalysts with tailored properties. Computer modelling is the most effective tool for such design.

Perhaps one of the most interesting and mysterious materials in nanocatalysis is gold. It has been believed that bulk gold is an inert noble metal that does not show any noticeable catalytic activity. However, in 1980s Haruta and Hutchings revealed that when the size of gold particles decreases to the nanoscale gold demonstrates extraordinary size-dependent catalytic activity and selectivity especially for the reactions involving O_2 .^[5-7] Since this discovery the number of theoretical and experimental groups working in the field of gold nanocatalysis is growing exponentially. Among many other scientists, we have been fascinated by such a miracle transformation from the inert to active^[8] and this fascination defined our further research activities for many years.

Gold nanocatalysis: tuning cluster reactivity by the size and morphology effects

We have started our work in the field of nanocatalysis with the classical and fundamental task – investigation on how simple molecules like oxygen and ethylene adsorb, become activated and interact with each other on small free neutral gold clusters.^[9] Our choice of ethylene was stipulated by the fact that C_2H_4 is the simplest alkene containing an isolated carbon-carbon double bond. Hence, it can be treated as a simple model molecule to study the epoxidation process of different alkenes.

[a] Global Research Center for Environment and Energy Based on Nanomaterials Science (GREEN), National Institute for Materials Science (NIMS), Tsukuba 305-0044, Japan
LYALIN.Andrey@nims.go.jp

[b] Department of Chemistry, Faculty of Science, Hokkaido University, Sapporo 060-0810, Japan

[c] Elements Strategy Initiative for Catalysts and Batteries (ESICB), Kyoto University, Kyoto 615-8245, Japan
take@sci.hokudai.ac.jp

Dr. Andrey Lyalin is a Special Researcher at the National Institute for Materials Science, Japan. He has been working in the area of atomic clusters and nanoparticles since 2000. His research interests are in the theoretical elucidation of various mechanisms affecting physical and chemical properties of materials at nanoscale, nanocatalysis and development of novel catalytic materials for energy and environment related applications.



Min Gao was born in Shandong, China, in 1986. She received her Ph.D. degree on the physical chemistry in 2012 from Hokkaido University under the supervision of Prof. Tetsuya Taketsugu. She then continued her research related catalytic reaction as a postdoctoral fellow until 2015. In 2016, she has become an assistant professor at quantum chemistry group in Hokkaido University. Her research interests include theoretical design of catalyst and mechanism study of catalytic reactions.



Tetsuya Taketsugu received his Ph.D. degree in theoretical chemistry from University of Tokyo in 1994 and became an assistant professor at the University of Tokyo in 1995. In 1999, he moved to Ochanomizu University as an associate professor and in 2005, he has become a professor of quantum chemistry group in Hokkaido University. His research interests focus on the development of new methodology to explore potential energy surfaces and reaction dynamics, as well as theoretical approach to design novel catalyst.



Using Density Functional Theory (DFT), we have demonstrated the appearance of the strong odd-even oscillations in the adsorption energy and O-O bond length of the adsorbed oxygen as a function of cluster size, as it is shown in Figure 2. These oscillations were explained with the use of the simple jellium model, which suggests that the gold clusters with an odd number of atoms have one unpaired electron over the closed-shell electronic structure. This unpaired electron can be easily transferred to the antibonding $2\pi^*$ orbital of O_2 , resulting in the strong activation of O_2 adsorbed on the gold clusters with the odd number of atoms (valence electrons). Such mechanism of the charge transfer-mediated activation of O_2 and odd-even variations in O_2 adsorption on metal clusters have been reported earlier; see, e.g.,^[10-16] and references therein. In turn, C_2H_4 can be adsorbed on small gold clusters in two different configurations, corresponding to the π - and di- σ bonded species^[17]. Adsorption in the π -bonded mode dominates over the di- σ mode over all considered cluster sizes up to 10 gold atoms, with the exception of the neutral C_2H_4 -Au₅ system, where the di- σ -bonded configuration is energetically more favorable, see Figure

2. There is striking difference in the size dependence of the binding energy of C_2H_4 to neutral gold clusters in the π and di- σ configurations. The binding energy of the π -bonded C_2H_4 develops non-monotonically as a function of cluster size with the local minima for Au₆. The binding energy, calculated for the di- σ -bonded C_2H_4 , exhibits pronounced odd-even oscillations (see Figure 2), showing the importance of the electronic shell effects in the di- σ mode of ethylene adsorption on gold clusters. Here and below the binding energy $E_b(M/S)$ of the molecule (particle) "M" to the cluster (surface) "S" is defined as

$$E_b(M/S) = E_{tot}(M) + E_{tot}(S) - E_{tot}(M/S), \quad (1)$$

where $E_{tot}(M/S)$ denotes the total energy of the compound system, while $E_{tot}(M)$ and $E_{tot}(S)$ are the total energies of the non-interacting molecule M and surface S, respectively.

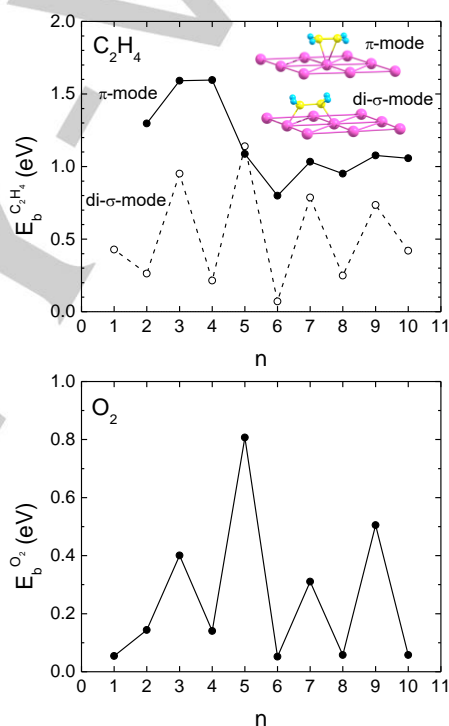


Figure 2. Binding energy, E_b , of O_2 and C_2H_4 molecules to neutral gold clusters with the number of atoms n up to 10. Both π (solid line) and di- σ (dashed line) modes of the adsorbed C_2H_4 are analyzed. DFT calculations are performed with the use of B3PW91 functional, and LANL2DZ (for Au) and aug-cc-pVTZ (for H, C, O) basis sets.

We have also demonstrated that the interaction of C_2H_4 with small gold clusters strongly depends on their charge. The excess of a positive or a negative charge on the gold cluster can change the balance between electron donation and back-donation processes. Hence, ethylene adsorption and reactivity can be manipulated by the cluster size and charge. This effect can be particularly important for understanding the mechanisms of catalytic activation of ethylene adsorbed on small gold

clusters. Adsorption of ethylene on gold clusters is accompanied by a weakening of the carbon-carbon double bond. This process concurs with the conventional activation of the adsorbed O_2 . Hence, activated dioxygen can readily attack the loosened double bond in C_2H_4 , thereby oxidizing the ethylene molecule. It is interesting that gold clusters mediate the interaction between the O_2 and C_2H_4 molecules, resulting in cooperative adsorption of dioxygen and ethylene.^[9]

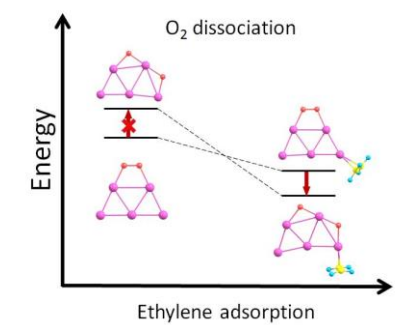


Figure 3. Reactant-promoted oxygen dissociation on gold clusters.

Therefore, we have suggested that the catalytic activity of gold clusters can be sensitive to the presence of adsorbates on the cluster surface, including the reactant molecule itself.^[18] In order to check this suggestion we performed a theoretical investigation of the molecular and dissociative adsorption of O_2 on the pure odd-size Au_n ($n = 1, 3, 5, 7, 9$) clusters and Au_n with a co-adsorbed reactant - ethylene molecule. We have demonstrated that catalytic activation of the adsorbed O_2 on the pure gold clusters in the size range considered is not sufficient for O_2 dissociation. However, the co-adsorption of C_2H_4 involves an extra charge transfer from the gold cluster to O_2 , which energetically promotes oxygen dissociation as shown in Figure 3. Thus the adsorption of the reactant molecule on the surface of small neutral gold clusters can considerably influence the oxygen-gold interaction, even when there is no direct interaction between oxygen and the reactant. Such a phenomenon sheds light on the basic understanding of the mechanisms of catalytic oxidation of ethylene and other hydrocarbons on gold clusters. Besides of the size and electronic structure, morphology effects can also affect considerably the catalytic activity of metal clusters. However, investigations on structural and morphology effects in nanocatalysis are rather scattered. Many theoretical studies on the reactivity of metal clusters consider only the most stable geometric structures as representative catalysts. On the other hand, gold nanoparticles possess large number of isomers having very close energies. Such structures can be fluxional at room temperature (possess transformations between these isomers) on a time scale typical for chemical reactions.^[15, 19-23] Therefore, it is rather questionable to consider only the most stable structures for description of the reactivity of cluster at finite temperatures. We were interested in such a phenomenon and wanted to understand how to describe in a systematic way chemical reactions occurring not only on the most stable cluster structures but also on the low-energy isomeric structures. In

other words we wanted to understand how to consider cluster reactivity in the regime of structural fluxionality. For this purpose in our group we introduced a new theoretical approach to find metal-cluster-catalyzed chemical bond activation pathways in the regime of structural fluxionality.^[24] This approach uses the global reaction route mapping (GRRM) technique combined with two automated reaction path search methods: the anharmonic downward distortion following (ADDF) and the artificial force induced reaction (AFIR) methods, developed recently by Maeda, Ohno and Morokuma.^[25]

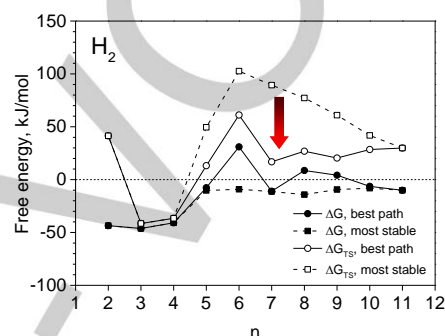


Figure 4. Change in free energy, ΔG , upon H_2 adsorption on the neutral gold clusters calculated for the most stable configurations (filled squares) and configurations leading to the best dissociation path (filled dots). Free energy of the lowest transition state for H_2 dissociation, ΔG_{TS} , calculated relative to the sum of free energies of the non-interacting H_2 and gold clusters for the most stable configurations (open squares) and configurations leading to the best dissociation path (open dots). DFT calculations are performed with the use of PBE functional and DZP basis sets.

Recently, we have performed systematic analysis of the structure-dependent cluster reactivity on the simple example of H_2 adsorption and dissociation on the small neutral and charged gold clusters.^[26] An exhaustive search of H_2 dissociation pathways has been performed not only on the most stable cluster structures but also on the large number of low energy isomers, allowing structural transformations between them. We presented strategy that can automatically identify the lowest transition states (TS) for H_2 dissociation with a systematic procedure. Temperature effects, cluster isomerization, and influence of the charge state of gold clusters on H_2 adsorption and dissociation have been studied. Figure 4 demonstrates that the presence of the isomer structures in the cluster ensemble results in a considerable decrease in TS energies for H_2 dissociation. It is amazing that for Au_5 , Au_7 , and Au_{10} clusters the energy difference between the most bounded structures and structures leading to the best dissociation path is very small (0.3–3.7 kJ/mol); however, in spite of this small difference, TS energy can be reduced dramatically. Namely, the relative free-energy values of ΔG_{TS} define the importance of various reaction pathways, as follows from the conventional transition-state theory. The appealing conclusion we made is that the most stable structures of the gold clusters are not always highly reactive. Therefore, the systematic search for reaction pathways accounting for contribution of all low-energy isomers is required

for an adequate description of H₂ dissociation on gold clusters. The novel approach we proposed in our group can serve as a promising tool for a systematic analysis and prediction of reactivity of small metal clusters in the regime of structural fluxionality.

Support effects in nanocatalysis: can inert support be really inert?

Interaction with the support is one of the most important factors in nanocatalysis.^[27, 28] So-called active supports, such as some of metal oxides, for example, MgO, ZnO, TiO₂, Al₂O₃, CeO₂, Fe₂O₃, etc. can considerably affect (enhance or suppress) the chemical properties, geometric structure and morphology of the supported nanoparticles.^[2, 10] Perimeter interface in the contact area of nanoparticles with the support often becomes a source of active sites for catalytic reactions;^[28-30] moreover charge transfer between the support and metal nanoparticles can lead to formation of the highly reactive charged clusters.^[31, 32]

It is also commonly accepted that so-called "inert" surfaces do not affect the electronic and geometry structure of the supported nanoparticles, and hence, such nanoparticles can be considered as pseudo-free. This suggestion is widely used to study intrinsic properties of metal nanoparticles that are free from the support effects.^[33] One of such "inert" supports, often used in experimental studies is hexagonal boron nitride (h-BN). Indeed, h-BN is an electrical insulator with a wide band gap and high thermal and chemical stability.^[34, 35] It is unlikely that such a support can influence the physical and chemical properties of the deposited metal nanoparticles.

However, the assumption about inert properties of BN support has not been verified until recently and very little attention has been paid to theoretical investigation concerning the role of h-BN in catalytic reactions. Such a gap in knowledge has stimulated our interest to the role of BN based materials in nanocatalysis. Using computer simulations, we wanted to confirm that h-BN is indeed an inert support for metal nanoparticles. Surprisingly, the results obtained have overcome all our expectations! We have found that BN based nanomaterials are not only able to modify the catalytic properties of the supported nanoparticles, but also can be functionalized and act as active catalysts.

As a first step, we have performed a systematic theoretical investigation of the structural, electronic, and catalytic properties of Au and Au₂ deposited on the pristine inert h-BN surface, as well as on the h-BN surfaces with boron vacancy (V_B), nitrogen vacancy (V_N), nitrogen impurity (N_B), and boron impurity (B_N) point defects. These simplest and relatively stable types of defects in h-BN are schematically shown in Figure 5.

The calculations are performed with the use of DFT with the gradient-corrected exchange-correlation functional of Wu and Cohen (WC) for two-layer h-BN slab containing 7x7 unit cells. Further details are described in [36, 37].

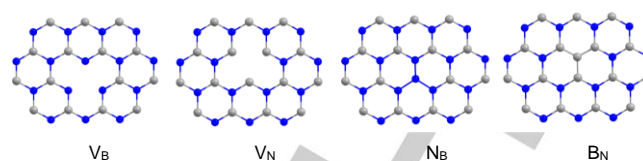


Figure 5. Schematic presentation of h-BN surface with boron vacancy (V_B), nitrogen vacancy (V_N), nitrogen impurity (N_B), and boron impurity (B_N) defects. Boron atoms are grey-colored and nitrogen atoms are dark blue.

We have selected the smallest gold particles Au and Au₂ as a simple model to elucidate the basic mechanisms of functionalization of gold on the inert h-BN support. The small free neutral gold clusters consisting of a few atoms are relatively inert toward O₂ activation and hence can serve as excellent model objects to study support effects. To obtain the most stable geometries of Au and Au₂ supported on the h-BN surface, we have created a large number of starting configurations by adding gold particles with the different orientations with respect to the surface. These structures have been fully optimized on the surface, with accounting for relaxation of all gold atoms as well as the top layer of h-BN. The bottom layer of h-BN in the slab was fixed. Thus, we have taken into account structural relaxations on the h-BN surface due to its interaction with the supported gold particles.

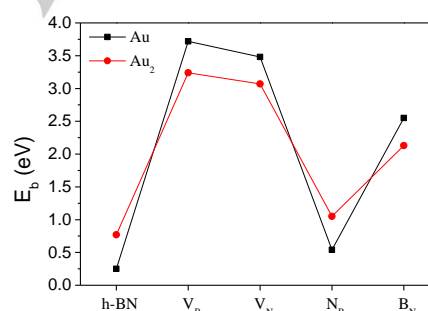


Figure 6. Calculated binding energy E_b of Au and Au₂ to the pristine and defected h-BN surfaces.

Figure 6 presents the results of our calculations of the binding energy of the gold particles to the defect-free and defected h-BN surface. Our calculations demonstrate that Au and Au₂ interact weakly with the pristine h-BN surface with the binding energies of 0.25 eV and 0.77 eV, respectively. However, the interaction of Au and Au₂ with the support becomes considerably stronger when the h-BN surface contains V_B, V_N, and B_N point defects. Thus, nitrogen and boron vacancy defects trap the gold atom with the binding energy of 3.48 and 3.72 eV, respectively. The gold dimer adsorbs on V_N and V_B with the binding energy of 3.07 and 3.24 eV, respectively.

There is a little charge transfer from the pristine *h*-BN surface to the adsorbed gold, but defected *h*-BN surface can act as a strong electron donor, as in the case of V_N , N_B , and B_N defects or electron acceptor, as for V_B defect. Figure 7 illustrates this effect on the example of Au atoms trapped by V_N and V_B vacancy defects in *h*-BN.

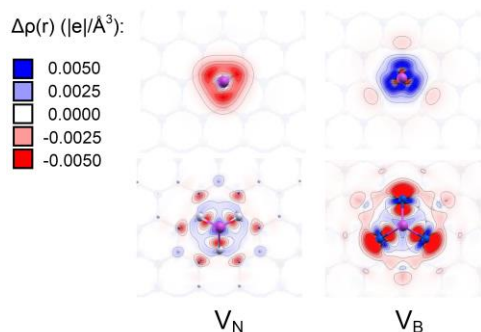


Figure 7. The electron density difference, $\Delta\rho = \rho(\text{Au}/h\text{-BN}) - \rho(\text{Au}) - \rho(h\text{-BN})$, induced by the interaction of Au with V_N and V_B vacancy defects in *h*-BN, and projected on the plane parallel to the *h*-BN surface passing through the adsorbed Au atom (upper row) and the plane passing through the corresponding vacancies in the *h*-BN surface (lower row). Blue and violet regions correspond to the electron loss, whereas red and pink regions correspond to the excess of the electron charge.

We have already mentioned that the charge state of metal particles affects their catalytic activity. As we can see now, even in the case of inert *h*-BN support it is possible to modify considerably the cluster's electron donor-acceptor capacity and its catalytic properties by the support design. Keeping this in mind, we have decided to check how O_2 molecule adsorbs on Au/*h*-BN systems and how *h*-BN support affects mechanism of oxygen activation. Can *h*-BN support really modify the catalytic properties of gold? Our calculations demonstrate that O_2 readily adsorbs on Au and Au_2 supported on the pristine and defected

h-BN surface, as shown in Figure 8.

As one can see from Figure 8, configurations of the adsorbed O_2 and the rate of catalytic activation (which can be estimated from the enlargement of the O-O bond length) are quite different for the different types of defects. Noticeably, that in the case of Au and Au_2 trapped by V_N center (which is a strong electron donor) O_2 bridges Au and the surface B atoms. Therefore, an interface between the supported gold particle and the *h*-BN surface might play an important role in catalytic reactions involving O_2 . We have shown that interaction of Au with the inert defect-free *h*-BN surface can lead to a dramatic change in the ability of gold to activate the adsorbed O_2 . In addition, the presence of the vacancy and impurity point defects on the *h*-BN surface results in a drastic change in the charge state of the trapped Au and Au_2 and hence also influences the catalytic activity of the supported gold particles.

Activation and reactivity of the adsorbed O_2 are strongly affected by the charge transfer from the gold hybridized 5d6s orbitals to the antibonding $2\pi^*$ orbital of O_2 . Although one can expect that the defected *h*-BN surface can influence the ability of the supported gold to activate the adsorbed O_2 , a similar effect found for the pristine *h*-BN surface is surprising. Bonding of Au to the defect-free *h*-BN surface is mainly driven by mixing of N- p_z with metal- d_{2z} orbitals and broadening of the 5d density of states of gold. In turn, such a broadening results in additional overlapping of the 5d states of Au with the 5σ and 1π states of the adsorbed O_2 .^[36] This effect leads to a strong additional mixing of the 5d states of Au with the 5σ and 1π states of O_2 . Thus, interaction of Au with the *h*-BN support promotes mixing of Au and O_2 states. Moreover, such an interaction leads to the population of the down-spin $2\pi^*$ orbital of O_2 and complete depopulation of the 6s orbital of Au. Population of the $2\pi^*$ state results in the additional activation of O_2 adsorbed on the Au/*h*-BN center in comparison with the free Au atom. Thus, interaction of Au with the defect-free *h*-BN surface leads to the strong promotion of binding and catalytic activation of the adsorbed O_2 . This is a rather surprising effect because it is widely believed that *h*-BN support is inert. Indeed, Au adsorbs weakly on the *h*-

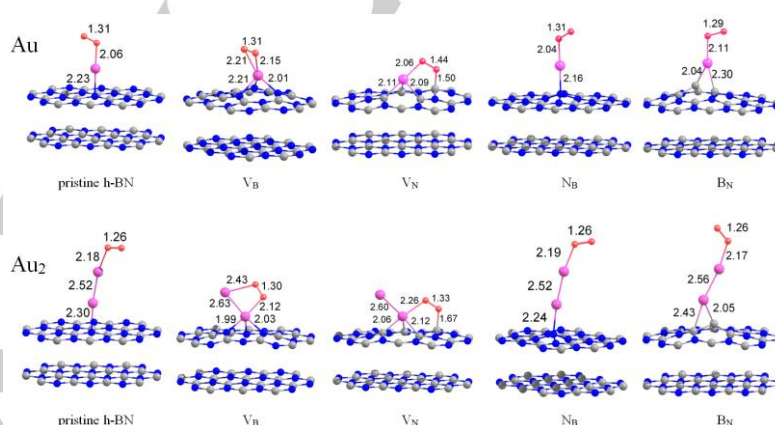


Figure 8. Optimized geometries of O_2 adsorbed on the supported Au (upper row) and Au_2 (lower row). The interatomic distances are given in \AA . Only part of the *h*-BN slab is shown.

BN surface and O₂ does not bind to *h*-BN at all. Nevertheless, mixing of the 5d states of the supported Au with N-p_z states of *h*-BN results in a strong modification of the Au-5d states, which in turn influence the adsorption and activation of O₂ on the supported Au. Such effect should also affect various processes of catalytic oxidation on the supported metal particles. In order to clarify our suggestion we have studied the model catalytic reaction of CO oxidation by molecular O₂ on Au atoms supported on the pristine and defected *h*-BN surface.^[38] We have found that O₂ binds stronger than CO on an Au atom supported on the defect free *h*-BN surface and *h*-BN surface with nitrogen vacancy V_N, but weaker than CO on a free Au atom or Au trapped by a boron vacancy V_B. The excess of the positive or negative charge on Au can considerably change its catalytic properties and enhance activation of the adsorbed O₂. Co-adsorption of CO and O₂ on the supported Au atom results in additional charge transfer to O₂. We have found that there are two different pathways for CO oxidation on the Au atom supported on *h*-BN surface: a two-step pathway where two CO₂ molecules are formed independently and a self-promotion pathway where oxidation of the first CO molecule is promoted by the second CO molecule. Interaction of Au with the defect-free and defected *h*-BN surface considerably affects the CO oxidation reaction pathways and barriers.^[36, 37] Our finding leads to a very important conclusion that Au supported on the *h*-BN surface (pristine or defected) cannot be considered as a pseudo-free atom. The support effects have to be taken into account, even when the interaction of Au with the support is weak.

From the inert support to effective electrocatalyst: magical transformation of boron nitride

The design of effective catalysts based on sustainable and abundant elements is an emerging problem. The oxygen reduction reaction (ORR) is one of the key processes in fuel cell technology where such a design is especially important.^[38] Currently the most efficient electrocatalysts for ORR are based on platinum. However, the high cost and limited resources of platinum prevent the wide use of fuel cells in practical applications for energy conversion.

Recently, it has been reported that carbon-based nanomaterials, such as graphene clusters or graphene sheets doped with nitrogen or nitrogen and boron atoms (carbon alloy catalyst), demonstrate high ORR activity.^[41-46] In such systems BN impurity pair can serve as an active site for ORR. This fact attracted our attention, because if consequently substitute all carbon atoms in graphene by boron and nitrogen one can get hexagonal boron nitride, which all consists of BN pairs. Can such material be an active catalyst for ORR? As we already discussed before, O₂ does not adsorb in the activated form on the pristine *h*-BN surface. Moreover, a catalyst for a fuel cell cathode must provide an electron transport to the active sites of the ORR. This is impossible when the catalyst has dielectric properties. These are the reasons why *h*-BN has never been considered as an ORR catalyst for fuel cells. However, we have already demonstrated that *h*-BN is not so inert as it was believed

before, and can affect catalytic properties of supported metal particles. Moreover, the band gap in a *h*-BN monolayer can be considerably reduced by vacancy and impurity defects.^[47-49] It was demonstrated experimentally that *h*-BN monolayer deposited on the transition metal support can be a conductor under certain conditions.^[50] It is important to note that adsorption energies of ORR intermediates can be strongly affected by the density of electronic states (DOS) near the Fermi level. Therefore a metal substrate or defects in *h*-BN can promote or affect the catalytic reactions on the *h*-BN surface. This suggestion motivated us for a search of possible ways to functionalize *h*-BN based nanosystems in order to act as active electrocatalysts for ORR.

The overall ORR can be written in a simple form as



A simple description of the ORR mechanism includes investigation on the adsorption preferences of O₂, OOH, O, and OH intermediates on a model catalyst and analysis of the overall energetics of the ORR process along the possible reaction pathways. A similar approach was used by Nørskov *et al.*^[51] and described in detail by Jacob and Keith.^[52-54]

To describe the energetics of the ORR, we analyzed the change in free energy, ΔG , along the reaction pathway, which can be done by calculating the heats of formation, ΔH_f , and accounting for the change in entropy, ΔS , during the reaction. To simulate the ORR under realistic conditions, it is also necessary to take into account zero-point-energy (ZPE) corrections, ΔE_{ZPE} , and the effect of the solvent (water) environment on the ORR process, ΔE_{water} . The overall change in free energy accounting for these corrections can be written as

$$\Delta G = \Delta H_f + \Delta E_{\text{ZPE}} - T\Delta S + \Delta E_{\text{water}} \quad (3)$$

where T is the temperature of the system. The heats of formation, ΔH_f , can be calculated using information on the binding preference and adsorption energies of the ORR intermediates. Detailed description of the procedure can be found in our recent works^[49, 55] and references therein.

First of all we have investigated possible ORR activity of *h*-BN monolayer modified with point defects. Similar to our previous works we have considered four simplest types of point defects in *h*-BN, namely nitrogen and boron impurities and vacancies, such as N_B, B_N, V_N, and V_B. Adsorption of the molecular oxygen is the first and one of the most important steps of ORR. We have demonstrated, that molecular oxygen chemisorbs on N_B, B_N, V_N, and V_B point defects in a singlet spin state with $E_b = 0.24$ eV, 1.62 eV, 3.10 eV, and 1.96 eV, respectively^[49]. Interaction of O₂ with the point defects in the *h*-BN monolayer results in activation of the adsorbed O₂ and weakening of the O–O bond. The calculated O–O bond length in O₂ adsorbed on N_B, B_N, and V_N defects is enlarged similar to the superoxide state of oxygen. In the case of O₂ adsorption on the V_B defect in the *h*-BN monolayer the oxygen molecule is partially dissociated with a distance between O atoms of 1.79 Å.

Can this adsorbed O_2 be active for the ORR? In general the ideal E_b of O_2 to a good catalytic material for the ORR should be as small as possible, but large enough to prevent O_2 from drifting away or desorbing from the catalytic center. We can also add that the heats of formation of the adsorbed O_2 should be smaller than the heats of formation of the OOH intermediate on the surface, otherwise the ORR will not be an energetically favorable process. Thus, in the case of Pt(111) surface, which is known to be a good catalyst for ORR, low temperature thermal desorption spectroscopy and electron energy-loss spectroscopy have determined E_b of the low-coverage O_2 to Pt(111) to be 0.3–0.5 eV.^[56–58] As we can see, although O_2 adsorbed on *h*-BN surface with B_N , V_N , and V_B defects is catalytically activated, the binding energy of O_2 to the support is too large. Therefore, a *h*-BN monolayer with B_N , V_N , and V_B defects cannot be a good catalyst for ORR. On the other hand, in the case of O_2 adsorption on the N_B impurity defect, the oxygen molecule is activated and weakly bounded to the surface. It is interesting that the binding energy of O_2 to N_B is similar to that known for O_2 adsorbed on the Pt(111) surface. Therefore, N doped *h*-BN monolayer can be a good candidate for ORR catalyst.

Another way to functionalize *h*-BN monolayer is to deposit it on a surface of some transition metals. Figure 9 shows that the partial DOS (PDOS) of *h*-BN monolayer adsorbed on Ni(111) is strongly modified due to interaction with the metal, demonstrating the appearance of the significant density of both occupied and unoccupied gap states with the N- p_z and B- p_z

characters. Such an effect occurs due to mixing of the Ni- d_{z^2} orbitals with N- p_z and B- p_z orbitals of the *h*-BN monolayer. One can also notice a spin polarization effect, which shifts the down-spin PDOS to the slightly higher energies and resulting in some differences in the up-spin and down-spin gap states.

In the case of Cu(111) and Au(111) surfaces the PDOS of the supported *h*-BN monolayer is also modified, but not so strong as for the Ni(111) surface. One can note appearance of the gap states at the top of the valence band of *h*-BN supported on Cu(111), but there are no gap states in the *h*-BN PDOS in the case of Au(111) support. We have also found a slight protrusion of the unoccupied BN states towards the Fermi level, clearly seen in the case of Cu(111) support and slightly noticeable in the case of Au(111). We have seen that the changes in PDOS of *h*-BN deposited on transition metal surfaces correlate with the strength of the *h*-BN-metal bonding, as it was already mentioned in [59].

The features of the electronic structure of *h*-BN monolayer supported on transition metal surfaces can affect the process of O_2 adsorption and activation. Indeed, the catalytic activation of the adsorbed O_2 is related to an electron transfer from the support to the anti-bonding $2\pi^*$ orbital of oxygen. Presence of defect levels or the gap states nearby the Fermi level can promote the electron transfer from the support to the adsorbed O_2 and hence result in its catalytic activation. Our calculations demonstrate that molecular oxygen physisorbs on the defect-free *h*-BN monolayer with the binding energy to the surface 0.06

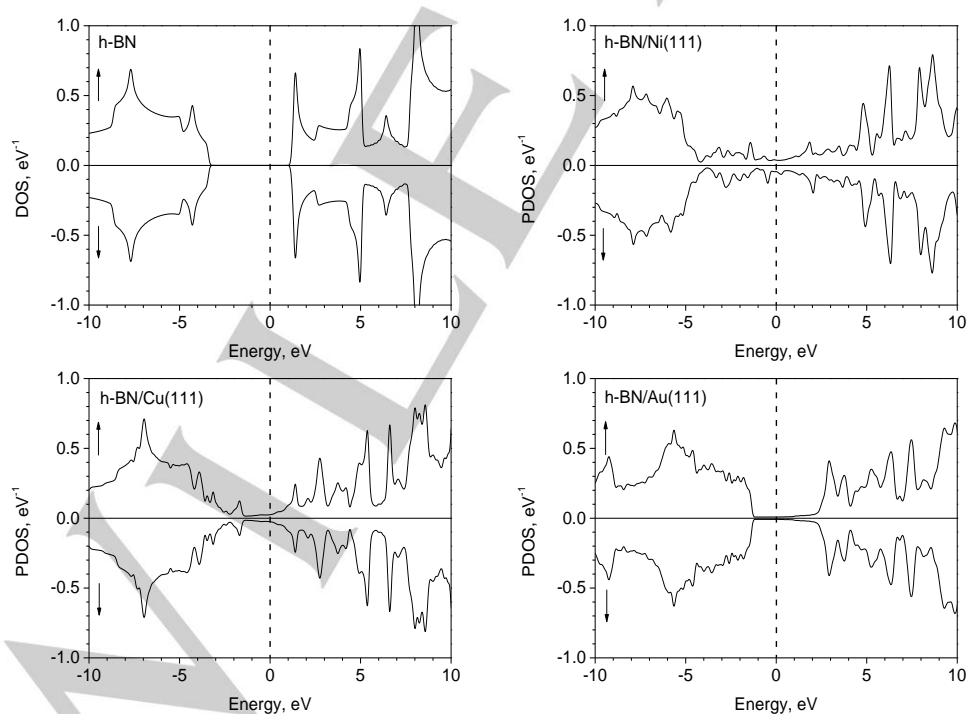


Figure 9. Spin polarized density of electronic states (DOS) calculated for the defect free *h*-BN monolayer as well as partial DOS (PDOS) projected on B and N atoms for *h*-BN/Ni(111), *h*-BN/Cu(111) and *h*-BN/Au(111) systems normalized by the number of BN pairs. The location of the Fermi level is indicated by a dashed vertical line at 0 eV. Arrows directed up and down indicate the up-spin and down-spin DOS, respectively. A Gaussian broadening of half-width 0.1 eV has been used.

eV. The physisorbed oxygen remains catalytically non-activated in its triplet state. The weak interaction of O_2 with the pristine *h*-BN monolayer is expected, as the defect-free *h*-BN is chemically inert material. However, Ni(111) and Cu(111) support strongly affects the chemical properties of *h*-BN monolayer and its ability to adsorb simple molecules. The results of our calculations show that molecular O_2 readily adsorbs on *h*-BN/Ni(111) in a top configuration (in a doublet spin state) with $E_b = 0.64$ eV and in a bridge configuration (in a singlet spin state) with $E_b = 1.51$ eV. It is interesting that adsorption preferences of O_2 on *h*-BN/Cu(111) and *h*-BN/Ni(111) surfaces are very similar.^[60] In the case of *h*-BN/Au(111) surface O_2 can only physisorb on the *h*-BN/Au(111) in a triplet inactivated state similar to the adsorption on the unsupported *h*-BN. However, we have found a metastable highly activated configuration of O_2 on *h*-BN/Au(111) with a binding energy of -0.05 eV. In this case O_2 binds to two B atoms nearest to the N atom sitting on top of Au in the first metal layer. As a result of formation of the metastable O_2 on the *h*-BN/Au(111) surface, the *h*-BN monolayer is strongly deformed and bends toward the metal surface. Therefore, adsorption of O_2 on *h*-BN/Au(111) can promote the local bonding of *h*-BN with Au(111). Finally, let us consider energetics of the ORR on defected and metal supported monolayer *h*-BN. Figure 10 presents the energy diagram calculated for the OOH association mechanism of the ORR on $N_B@h$ -BN and *h*-BN/Ni(111) systems.^[49, 55] Heats of formation, ΔH_f , without ZPE and solvent corrections are presented by dashed lines, whereas changes in free energy, ΔG , accounting for entropy, zero-point-energy, and solvent effects are presented by solid lines. Heats of formation along the reaction pathway were obtained in the approximation of the independent adsorption of ORR intermediates, which is a good approximation in the case of low coverage on the catalytic surface, as considered in the present work. It is interesting that ΔE_{ZPE} and $-T\Delta S$ terms in the expression for the free energy destabilize the system; while accounting for a water environment results in considerable stabilization of ORR intermediates. The absolute values of energy corrections are large. However, ΔE_{ZPE} , $-T\Delta S$, and ΔE_{water} corrections partly cancel each other. Thus the total contribution of all considered corrections to the free energy is relatively small. Therefore, in order to reproduce the energetics of the ORR process correctly it is important to take into account zero-point energy, entropy and solvent effects simultaneously.^[49]

It is seen from Figure 10 that in the case of N-doped *h*-BN monolayer all steps of ORR process are energetically favorable. However, for *h*-BN/Ni(111) system the uncorrected ΔH_f value goes downhill until formation of two OH^* moieties on *h*-BN/Ni(111), whereas the further reduction of $2OH^*$ to $2H_2O$ is unfavorable energetically as a result of strong OH^* binding to *h*-BN/Ni(111). Nevertheless, accounting for entropy, zero-point energy, and solvent effects makes the last step of the ORR process energetically favorable. The reason for the drop in ΔG calculated for the last step of the ORR is the considerable decrease in the destabilization term $-T\Delta S$ due to the fact that the final product of the reaction, $2H_2O$, does not bind to the surface, so that its entropy is not zero. The calculated value of the standard Gibbs free energy of formation of one H_2O

molecule in the liquid phase is -2.95 eV, which slightly overestimates the experimental value of -2.46 eV. Figure 10 shows that ΔG decreases along the whole reaction pathway, making the ORR on N-doped *h*-BN and *h*-BN/Ni(111) possible. This very important result demonstrates clearly that a chemically inert material, such as *h*-BN, can be functionalized and become catalytically active for the ORR. Unfortunately, neither N-doped monolayer *h*-BN, nor *h*-BN/Ni(111) system are good materials for the real electrochemical applications in fuel cell. N-doped *h*-BN is not a conductor, while Ni is not stable in the potential region close to the onset of ORR and, therefore, not a good substrate for the cathode material in fuel cell. On the other hand Au(111) substrate is stable and poor ORR catalyst. Therefore it is an ideal substrate to verify properties of BN bases nanomaterials for ORR activity. Moreover, we have demonstrated that metastable O_2 can be highly activated on *h*-BN/Au(111) surface. Therefore, *h*-BN/Au(111) is a good system for further theoretical and experimental study of ORR activity.

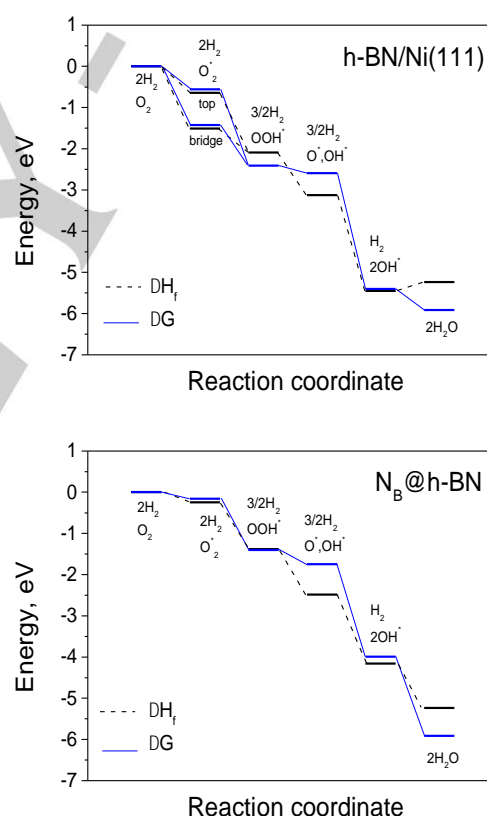


Figure 10. Energy diagram for the ORR on N-doped *h*-BN and *h*-BN/Ni(111), including heats of formation, ΔH_f (dashed line), and changes in free energy, ΔG , accounting for entropy, zero-point energy, and solvent effects (solid line). In the case of *h*-BN/Ni(111), both the on-top (superoxo-like) and bridge (peroxo-like) configurations of the adsorbed O_2 are considered.

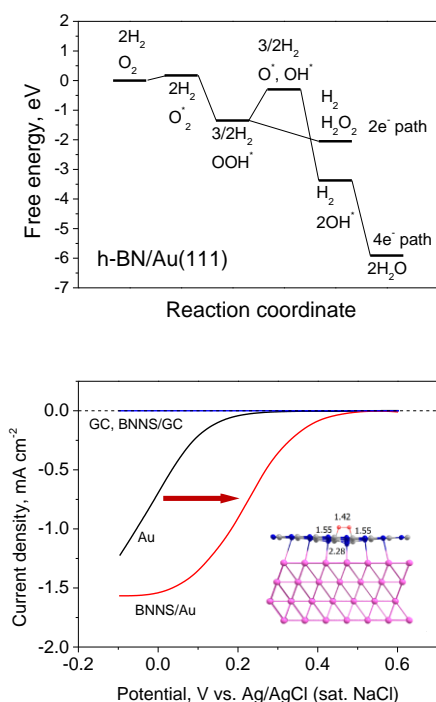


Figure 11. Free energy diagram for ORR on the *h*-BN/Au(111) and LSVs of bare Au, BNNS/Au, bare GC, and BNNS/GC in O₂ saturated 0.5 M H₂SO₄. Inset: Optimized structure of the metastable O₂ on the *h*-BN/Au(111) surface with the distances given in Å.

Figure 11 demonstrates free energy diagrams for ORR at the *h*-BN/Au(111) surface accounting for entropy contribution, zero-point energy corrections, and solvent effects on the adsorption energies of O₂ and all ORR intermediates with the assumption of independent adsorption of ORR intermediates.^[61] Two processes, i.e., a four-electron process via OOH producing water and a two-electron process producing H₂O₂, are considered. It is clear that while the dissociation of OOH* to O* and OH* leading to the four-electron process is not energetically favorable, the reduction of OOH* to H₂O₂ is possible. Such mechanism is quite different from N-doped *h*-BN and *h*-BN/Ni(111) systems where dissociation of OOH* is energetically favorable. Nevertheless, our theoretical prediction clearly suggests that BN on Au can act as an electrocatalyst for ORR. Such a finding has stimulated experimental verification of the obtained results. Experiments have been performed in the group of Uosaki. Figure 11 shows the linear sweep voltammograms (LSVs) of bare and BN nano-sheet (BNNS) modified Au electrodes obtained in an O₂ saturated 0.5 M H₂SO₄ solution in a rotating disk electrode configuration. The potential was scanned from +0.6 to -0.1 V. It is clear that BNNS acts as an electrocatalyst for ORR as the overpotential is reduced by ca. 0.27 V if BNNS is placed on Au. The number of electrons involved in ORR determined from the slope of Levich plot is ca. 2, showing the ORR product is H₂O₂, at both the bare and BNNS modified Au electrode.^[61] To examine the effect of the substrate, ORR behaviors of bare and BNNS modified glassy carbon (GC)

electrodes were also measured under the same conditions used for Au electrodes. A GC substrate was chosen because theoretical calculation shows that graphite support does not affect electronic structure of the supported monolayer of *h*-BN and BNNS/graphite is not active for O₂ adsorption. In contrast to the results at the Au substrate, almost no electrocatalytic activity was observed at both the bare and BNNS modified GC electrode, confirming the important role of the Au substrate for the activation of BNNS for the ORR catalyst.^[59]

Where are the active sites for ORR? The above calculations for O₂ adsorption and the free energy diagram are performed for the terrace of *h*-BN/Au(111). However, a current sensing atomic force microscopy (AFM) study showed that the BN on Au was not very conductive even when the thickness of the BNNS was ~0.9 nm, suggesting that the edge region of *h*-BN islands of finite size or nanosheets (BNNS) is more favorable for ORR than the terrace. Therefore we have performed additional calculations and demonstrated that O₂ readily adsorbs in the highly activated form at the edge of BN island on Au(111) surface with the binding energy of 0.2–0.4 eV, while O₂ remains metastable at the BNNS terrace.^[61] This suggests the importance of the edge of BNNS as an ORR site, although more detailed experimental and theoretical investigations on this problem are required to define actual mechanism of ORR on *h*-BN/Au(111) system.

Our analysis suggests exciting ways for a rational design of novel catalytic materials on the base of theoretical modelling followed by experimental verification, where theory suggests and experiment confirms or corrects theoretical prediction. In such an approach theory leads the process of discovery of new materials. Thus, our theoretical analysis of the possible adsorption sites of ORR intermediates on the terrace or edge of BNNS on Au(111) surface suggests that edges of BNNS can be more active for ORR and hence in order to increase the electrocatalytic activity of BNNS/Au system one should decrease the size of BNNS islands, which would increase the edge/surface relative proportion and overall catalytic activity. This suggestion requires urgent experimental verification. Moreover, it is clear from the analysis of free energy diagram presented in Figure 11 that four-electron pathway for ORR on the BNNS terrace is not possible due to the lack of stability of O* and OH* intermediates. Therefore, one can suggest that providing additional sites for stabilization of oxygen on BNNS/Au(111) would promote the effective 4-electron pathway of ORR with formation of H₂O. Gold nanoparticles supported on BNNS/Au are excellent candidates to provide such active sites for O₂ adsorption. To confirm this suggestion and gain further insight into mechanism of ORR on BNNS/Au(111) system we have performed theoretical analysis of a free energy profile for all intermediates of ORR on the model system consisting of a small Au₈ cluster supported on BNNS/Au(111).^[62] A free neutral Au₈ cluster is inert towards adsorption and activation of O₂ possessing enhanced stability due to the electronic shell closure effect. However, being supported on BNNS/Au surface, small charge transfer from Au₈ to the support breaks cluster electronic shell closure promoting interaction with molecular and atomic oxygen. Therefore, small gold nanoparticle on BN/Au provides active sites for oxygen adsorption which promotes OOH

dissociation opening the route to effective 4-electron pathway of ORR, as shown in Figure 12.

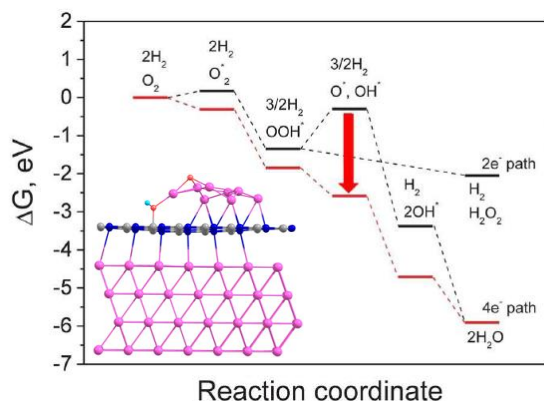


Figure 12 Free energy diagrams for ORR at BNNS/Au(111) (black line) and Au₈@BNNS/Au(111) (red line) electrodes and optimized geometry of the dissociated OOH on Au₈@BNNS/Au(111).

Our calculations demonstrate that while Au₈ cluster on BNNS/Au(111) mildly stabilizes O₂^{*}, OOH^{*} and OH^{*} intermediates by 0.5 – 0.7 eV, it drastically stabilizes O^{*} by 1.6 eV in comparison with the adsorption at BNNS/Au(111) surface. Such stabilization of O^{*} on Au₈@BNNS/Au(111) makes the dissociation of OOH^{*}, which is an uphill process at BNNS/Au(111) surface, downhill, opening a 4-electron reduction pathway of oxygen to H₂O. Such theoretical interpretation has been confirmed experimentally, where it was shown that gold nanoparticle decoration of insulating boron nitride on inert gold electrode forms an efficient electrocatalyst for the ORR.^[62] Although the h-BN/Au(111) system is not as active as Pt for ORR, our combined theoretical and experimental investigation demonstrates the possibility to functionalize completely inert materials to become ORR catalysts, opening new ways to design effective Pt-free catalysts for FC based on the principally new materials never considered before as catalysts.

Summary and Outlook

In this personal account we have shared our experience related to the theoretical design of effective catalysts for environment and energy related applications. We have described our exciting journey from the realm of gold nanocatalysis to the new and yet unexplored land of the boron nitride or non-traditional materials catalysis. The main idea that stands behind of our work is that even catalytically inactive or completely inert materials can be functionalized at nanoscale via the size, structure, morphology and support effects. Our research has been strongly influenced by the field of gold nanocatalysis with its fascinating transformation of the noble gold from the inert to the highly reactive form at nanoscale. However, gold is certainly not the only material that can show such transformation. Thus we have found that chemically inert hexagonal boron nitride is not actually inert and can affect catalytic properties of the supported

metal particles. Moreover, inert boron nitride demonstrates extraordinary catalytic properties itself when in contact with transition metals, in particular with the inert gold surface. The larger story can be learned from this research – search for the novel effective catalytic materials should not be limited by the traditional elements with well-known catalytic properties. Materials that have never been considered as possible catalysts can demonstrate magical transformation of their properties by analogy with gold or boron nitride. Special attention should be paid to possibility to emerge catalytically active sites by forming contact of two inert compounds. We believe that such approach opens principally new ways to design catalytically active systems based on materials never before been considered as catalysts. In all the examples provided it is clear that materials at nanoscale possess absolutely unique properties that are not possible to understand without systematic theoretical analysis. The primary aim of our work is to learn how to predict and design nanocatalysts with the desirable properties based on computer modelling and simulations. We believe that in the nearest future such computer based experiments will be the main tool for the effective design of novel materials.

Acknowledgements

This work was supported by the Japan Society for the Promotion of Science (JSPS KAKENHI Grants 15K05387 and 26288001), the FLAGSHIP2020 program supported by the Ministry of Education, Culture, Sports, Science and Technology (MEXT), Japan within the priority study5 (Development of new fundamental technologies for high-efficiency energy creation, conversion/storage and use) and partly performed under the management of the "Elements Strategy Initiative for Catalysts and Batteries (ESICB)" supported by MEXT program Elements Strategy Initiative to Form Core Research Center" (since 2012). The present work was partially supported by the Development of Environmental Technology using Nanotechnology from MEXT. The computations were partly performed at the Research Center for Computational Science, Okazaki, Japan.

Keywords: *h*-BN • catalyst • gold clusters • oxygen reduction reaction • nanocatalysis

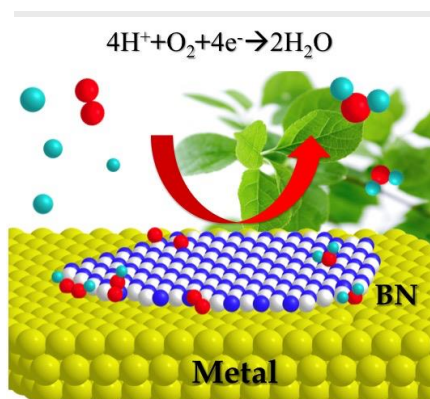
References

- [1] P. Serp and K. Philippot, *Nanomaterials in Catalysis, First Edition*. Wiley-VCH Verlag GmbH & Co. KGaA, **2013**.
- [2] U. Heiz, U. Landman, *Nanocatalysis*; Springer: Berlin, Heidelberg, New York, **2007**.
- [3] J. K. Nørskov, T. Bligaard, J. Rossmeisl and C. H. Christensen, *Nature Chemistry* **2009**, *1*, 37-46.
- [4] A. R. Oganov and C. W. Glass, *J. Chem. Phys.* **2006**, *124*, 244704.
- [5] M. Haruta, T. Kobayashi, H. Sano and N. Yamada, *Chem. Lett.* **1987**, *16*, 405-408.
- [6] M. Haruta, *Catalysis Today*, **1997**, *36*, 153-166.
- [7] A. S. K. Hashmi and G. J. Hutchings, *Angew. Chem. Int. Ed.*, **2006**, *45*, 7896-7936.
- [8] A. Sanchez, S. Abbet, U. Heiz, W.-D. Schneider, H. Häkkinen, R. N. Barnett, and U. Landman, *J. Phys. Chem. A* **1999**, *103*, 9573-9578.
- [9] A. Lyalin and T. Taketsugu, *J. Phys. Chem. C* **2009**, *113*, 12930-12934.

- [10] R. Coquet, K. L. Howard and D. Willock, *J. Chem. Soc. Rev.* **2008**, 37, 2046.
- [11] X. Ding, Z. Li, J. Yang, J. G. Hou, and Q. Zhu, *J. Chem. Phys.* **2004**, 120, 9594.
- [12] E. M. Fernández, P. Ordejón and L. C. Balbás, *Chem. Phys. Lett.* **2005**, 408, 252.
- [13] H. Häkkinen and U. Landman, *J. Am. Chem. Soc.* **2001**, 123, 9704–9705.
- [14] L. D. Socaciu, J. Hagen, T. M. Bernhardt, L. Wöste, U. Heiz, H. Häkkinen, and U. Landman, *J. Am. Chem. Soc.* **2003**, 125, 10437–10445.
- [15] H. Häkkinen, S. Abbet, A. Sanchez, U. Heiz and U. Landman, *Angew. Chem. Int. Ed.* **2003**, 42, 1297–1300.
- [16] B. Yoon, H. Häkkinen, U. Landman, *J. Phys. Chem. A* **2003**, 107, 4066–4071.
- [17] A. Lyalin and T. Taketsugu, *J. Phys. Chem. C* **2010**, 114, 2484–2493.
- [18] A. Lyalin and T. Taketsugu, *J. Phys. Chem. Lett.* **2010**, 1, 1752–1757.
- [19] L. Barrio, P. Liu, J. A. Rodríguez, J. M. Campos-Martín, J. L. G. Fierro, *J. Chem. Phys.* **2006**, 125, 164715.
- [20] Vargas, A.; Santarossa, G.; Iannuzzi, M.; Baiker, A. *Phys. Rev. B* **2009**, 80, 195421.
- [21] P. Koskinen, H. Häkkinen, B. Huber, B. Von Issendorff, M. Moseler, *Phys. Rev. Lett.* **2007**, 98, 015701.
- [22] X. Gu, S. Bulusu, X. Li, X. C. Zeng, J. Li, X. G. Gong and L.-S. Wang, *J. Phys. Chem. C* **2007**, 111, 8228–8232.
- [23] Z. Y. Li, N. P. Young, M. Di Vece, S. Palomba, R. E. Palmer, A. L. Bleloch, B. C. Curley, R. L. Johnston, J. Jiang, J. Yuan, *Nature* **2008**, 451, 46–48.
- [24] M. Gao, A. Lyalin, S. Maeda, and T. Taketsugu, *J. Chem. Theory Comput.* **2014**, 10, 1623–1630.
- [25] S. Maeda, K. Ohno and K. Morokuma, *Phys. Chem. Chem. Phys.* **2013**, 15, 3683–3701.
- [26] M. Gao, A. Lyalin, M. Takagi, S. Maeda, and T. Taketsugu, *J. Phys. Chem. C*, **2015**, 119, 11120–11130.
- [27] G. C. Bond and D. T. Thompson, *Gold Bull.* **2009**, 42, 247.
- [28] M. Haruta, *Faraday Discuss.* **2011**, 152, 11.
- [29] A. Lyalin, T. Taketsugu, *Faraday Dis.* **2011**, 152, 185.
- [30] M. Gao, A. Lyalin, T. Taketsugu, *Catalysts* **2011**, 1, 18.
- [31] B. Yoon, H. Häkkinen, U. Landman, A. S. Wörz, J.-M. Antonietti, S. Abbet, K. Judai, and U. Heiz, *Science*, **2005**, 307, 403.
- [32] M. Chen, Y. Cai, Z. Yan, D. W. Goodman, *J. Am. Chem. Soc.* **2006**, 128, 6341.
- [33] M. Turner, V. B. Golovko, O. P. H. Vaughan, P. Abdulkhin, A. Berenguer-Murcia, M. S. Tikhov, B. F. G. Johnson and R. M. Lambert, *Nature* **2008**, 454, 981.
- [34] R. Arenal, O. Stéphan, M. Kociak, D. Taverna, A. Loiseau and C. Colliex, *Phys. Rev. Lett.* **2005**, 95, 127601.
- [35] D. Golberg, Y. Bando, Y. Huang, T. Terao, M. Mitome, C. Tang and C. Zhi, *ACS Nano* **2010**, 4, 2979.
- [36] M. Gao, A. Lyalin, and T. Taketsugu, *J. Phys. Chem. C* **2012**, 116, 9054–9062.
- [37] M. Gao, A. Lyalin, and T. Taketsugu, *Int. J. Quantum Chem.* **2013**, 113, 443–452.
- [38] M. Gao, A. Lyalin, and T. Taketsugu, *J. Chem. Phys.* **2013**, 138, 034701.
- [39] M. Gao, A. Lyalin, and T. Taketsugu, *J. Phys.: Conf. Ser.* **2013**, 438, 012003.
- [40] V. R. Stamenkovic, B. Fowler, B. S. Mun, G. F. Wang, P. N. Ross, C. A. Lucas and N. M. Markovic, *Science* **2007**, 315, 493.
- [41] R. A. Sidik, A. B. Anderson, N. P. Subramanian, S. P. Kumaraguru and B. N. Popov, *J. Phys. Chem. B*, **2006**, 110, 1787–1793.
- [42] J.-i. Ozaki, T. Anahara, N. Kimura and A. Oya, *Carbon*, **2006**, 44, 3358–3361.
- [43] T. Ikeda, M. Boero, S.-F. Huang, K. Terakura, M. Oshima and J.-i. Ozaki, *J. Phys. Chem. C*, **2008**, 112, 14706–14709.
- [44] T. Ikeda, M. Boero, S.-F. Huang, K. Terakura, M. Oshima, J.-i. Ozaki and S. Miyata, *J. Phys. Chem. C*, **2010**, 114, 8933–8937.
- [45] L. Yu, X. Pan, X. Cao, P. Hu and X. Bao, *J. Catal.*, **2011**, 282, 183–190;
- [46] L. Qu, Y. Liu, J.-B. Baek and L. Dai, *ACS Nano*, **2010**, 4, 1321–1326.
- [47] H. Zeng, C. Zhi, Z. Zhang, X. Wei, X. Wang, W. Guo, Y. Bando and D. Golberg, *Nano Lett.*, **2010**, 10, 5049–5055.
- [48] S. Azevedo, J. R. Kaschny, C. M. de Castilho and F. de Brito Mota, *Eur. Phys. J. B*, **2009**, 67, 507–512.
- [49] A. Lyalin, A. Nakayama, K. Uosaki and T. Taketsugu, *Phys. Chem. Chem. Phys.*, **2013**, 15, 2809–2820.
- [50] A. B. Preobrajenski, A. S. Vinogradov and N. Mårtensson, *Surf. Sci.* **2005**, 582, 21–30.
- [51] J. K. Nørskov, J. Rossmeisl, A. Logadottir, L. Lindqvist, Kitchin, J. R. T. Bligaard, H. Jónsson, *J. Phys. Chem. B* **2004**, 108, 17886–17892.
- [52] J. A. Keith, G. Jerkiewicz and T. Jacob, *Chem. Phys. Chem.* **2010**, 11, 2779–2794.
- [53] T. Jacob, *Fuel Cells* **2006**, 06, 159–181.
- [54] J. A. Keith and T. Jacob, *Angew. Chem., Int. Ed.* **2010**, 49, 9521–9525.
- [55] A. Lyalin, A. Nakayama, K. Uosaki, and T. Taketsugu, *J. Phys. Chem. C* **2013**, 117, 21359–21370.
- [56] J. L. Gland, B. A. Sexton and G. B. Fisher, *Surf. Sci.*, **1980**, 95, 587–602.
- [57] C. Campbell, G. Ertl, H. Kuipers and J. Segner, *Surf. Sci.*, **1981**, 107, 220–236.
- [58] P. D. Nolan, B. R. Lutz, P. L. Tanaka, J. E. Davis and C. B. Mullins, *J. Chem. Phys.*, **1999**, 111, 3696–3704.
- [59] R. Laskowski, P. Blaha, K. Schwarz, *Phys. Rev. B* **2008**, 78, 045409.
- [60] A. Lyalin, A. Nakayama, K. Uosaki and T. Taketsugu, *Top Catal.* **2014**, 57, 1032–1041.
- [61] K. Uosaki, G. Elumalai, H. Noguchi, T. Masuda, A. Lyalin, A. Nakayama, and T. Taketsugu, *J. Am. Chem. Soc.* **2014**, 136, 6542–6545.
- [62] G. Elumalai, H. Noguchi, A. Lyalin, T. Taketsugu, K. Uosaki, *Electrochem. Commun.* **2016**, 66, 53–57.

PERSONAL ACCOUNT

Inert nonconductive hexagonal boron nitride sheet on inert gold surface acts as an effective electrocatalyst for oxygen reduction reaction



Andrey Lyalin*, Min Gao, Tetsuya Taketsugu*

Page xxx. – Page xxx.

When inert becomes active:
fascinating route for catalyst design